Proceedings of the 2003 IEEE International Frequency Control Symposium and PDA Exhibition
Jointly with the 17th European Frequency and Time Forum

CAVITY-Q AGING IN THE GAS-CELL ATOMIC CLOCK: STUDIES WITH AN ATOMIC-CANDLE SIGNAL

James Camparo
Electronics and Photonics Laboratory, The Aerospace Corporation
Mail Stop: M2-253, PO Box 92957, Los Angeles, CA 90009

Abstract - **Slow variations in cavity Q and microwave power are thought to play a role in the long-term frequency stability of gas-cell atomic clocks. Here, we use an atomic-*candle* method to study the aging of a TE_{011} microwave cavity's resonant frequency and quality factor when a glass resonance cell containing Rb^{87} loads the cavity. Our results suggest that the alkali vapor coats the inside glass surface of the resonance cell with a thin metallic film, and that as this film evolves the quality factor degrades. More generally, the present work demonstrates the efficacy of the atomic-candle method for investigating cavity resonances. In particular, we show that when used in conjunction with more traditional methods, the atomic-candle method has the potential to reveal information on a cavity mode's spatial profile.**
Keywords - **Gas-cell clock, atomic candle, microwave cavity**

I. INTRODUCTION

Though well documented, it is not always appreciated that the gas-cell atomic clock's output frequency depends on the electrical characteristics of the clock's microwave cavity, specifically the cavity's resonant frequency, ω_c, and quality factor, Q_c. Two mechanisms are primarily responsible for this sensitivity, the position-shift effect [1,2] and a cavity-pulling effect [3]. (These effects are briefly discussed in the Appendix.) As a consequence, since the late eighties there have been recurring suggestions that the long-term stability of gas-cell clocks might be influenced by the microwave cavity [4,5]. It therefore comes as a surprise to find a dearth of studies in the open literature dealing with this issue. While some authors have considered the magnitude of the cavity-pulling effect [6,7], and others have considered the design of compact, dielectrically loaded cavities for miniaturized devices [8-10], we know of no studies addressing potential deterministic/stochastic variations of either ω_c or Q_c in the gas-cell clock. Of course, it is well known that for an unloaded microwave cavity ω_c will change in response to the cavity's temperature, primarily as a result of thermal expansion [11]. However, in the case of gas-cell clocks the resonance cell loads the microwave cavity. Since the resonance cell contains an alkali vapor, the cell's inside glass surface will become coated with a thin conducting metallic film [12], and this could lead to a non-negligible increase in the rate at which modal field energy is lost. Consequently, one could easily imagine the loaded cavity's resonant frequency and quality factor changing as a rubidium film slowly evolved on the resonance cell's inner surface.

In this work, we describe experiments examining the temporal behavior of a microwave cavity's resonant frequency and quality factor when loaded by an alkali-containing glass resonance cell. To this end, we have taken advantage of the atoms' atomic-*candle* signal [13], which is an atomic measure of microwave field strength [14]. With our atomic-candle method we are able to probe the field inside the cavity *at the location where the atoms generate the atomic clock signal* (i.e., we perform a local measurement of field strength). In more standard techniques for studying cavity resonances (e.g., transmitted power methods [15]), global cavity field strength is measured. In the following section we describe the atomic-candle signal and our experimental method. Then, in Section III, we report on the long-term aging of ω_c and Q_c due to what we hypothesize is a redistribution of rubidium metal within the resonance cell. We conclude with a discussion of the atomic clock stability issues raised by our findings.

II. ATOMIC-CANDLE METHOD FOR MEASURING A CAVITY'S RESONANCE

Over the past decade, researchers have come to recognize that atomic systems can exhibit parametric or "Rabi-resonances" [16,17], where this particular type of resonant behavior arises from an atom's interaction with a modulated field. Briefly, the modulated field induces atomic population oscillations, and the amplitude of these oscillations, δ_{pop}, exhibits resonance when the field's modulation frequency, ω_m, matches the atom's Rabi frequency, Ω [18].[1] There are at least two different types of Rabi-resonance [13], and one of these finds application in a device called an atomic candle, where field amplitude is locked to the peak of the Rabi-resonance in much the same way as field frequency is stabilized in an atomic clock [19,20]. As

1) For the magnetic dipole transition considered here, $\Omega = \mu_B B/\hbar$, where μ_B is the Bohr magneton and B is the microwave magnetic field amplitude.

discussed elsewhere [13], the atomic-candle signal has the form:

$$\delta_{pop} \sim \frac{\hbar^2\omega_m\Omega^2\gamma_2\left[\gamma_2^2+\left(\frac{\gamma_2}{\gamma_1}\right)\Omega^2\right]^{-1}}{\sqrt{\left(\mu_B^2B^2-4\hbar^2\omega_m^2\right)^2+4\hbar^4\gamma_1^2\omega_m^2}}, \qquad (1)$$

where γ_1 and γ_2 are the longitudinal and transverse atomic relaxation rates, respectively. This signal is illustrated in Fig. 1a, where experimental values of δ_{pop} are plotted as a function of the microwave magnetic field strength in our cavity. (Our method for measuring δ_{pop} will be discussed more fully below.) As the figure shows, there is a sharp resonant increase in δ_{pop} when $B = B_{res} = 2\hbar\omega_m/\mu_B$.[2] With regard to present considerations, Fig. 1a indicates that atoms can act as *sensors* of electromagnetic field strength via their atomic-candle signals: for a specific value of the modulation frequency, the maximum value of δ_{pop} occurs at a unique value of the cavity's field strength. Fig. 1b illustrates how we employed this idea to measure a microwave cavity's resonant frequency and quality factor.

For an ideal cylindrical TE_{mnp} cavity mode excited by a fixed microwave frequency (e.g., the ground-state hyperfine transition frequency of Rb^{87}, $\omega_{hfs}/2\pi =$ 6834.7 MHz) the field energy in the cavity, B^2, can be written as [21]

$$B^2 = \frac{\left(\frac{\omega_{hfs}}{2Q_c}\right)^2 B_o^2}{\left(L-L_{mnp}\right)^2\frac{(\pi pc)^4}{\omega_{hfs}^2L_{mnp}^6}+\left(\frac{\omega_{hfs}}{2Q_c}\right)^2}. \qquad (2)$$

Here, L is the cavity length; L_{mnp} is the specific length associated with the mnp-mode's resonance (for input frequency ω_{hfs}), and B_o^2 is the resonant field energy in the cavity. Note that B_o^2 is proportional to the setting of the external attenuator (expressed as a signal gain factor), G. Employing a microwave field with relatively slow phase modulation (i.e., $\omega_m/2\pi = 10^2$-10^3 Hz), we induce atomic population oscillations, and, for a particular value of L, adjust the external gain so as to maximize the amplitude of the atomic population oscillations. Considering Eq. (1), we "tune" B (via G) to the atomic-candle signal's peak. For this level of external gain, Eq. (1) indicates that $B(L) = 2\hbar\omega_m/\mu_B$, and we label this particular gain as G_{res}. Since $B_o^2 \sim G$, we can rearrange Eq. (2) to yield

$$\frac{1}{G_{res}} \sim \frac{\left(\frac{\mu_B}{2\hbar\omega_m}\right)^2\left(\frac{\omega_{hfs}}{2Q_c}\right)^2}{\left(L-L_{mnp}\right)^2\frac{(\pi pc)^4}{\omega_{hfs}^2L_o^6}+\left(\frac{\omega_{hfs}}{2Q_c}\right)^2}, \qquad (3)$$

where we have approximated L_{mnp} with the nominal cavity length L_o in the factor that multiplies the cavity-length term in the denominator. Thus, a plot of G_{res}^{-1} as a function of L yields the cavity resonance lineshape, and allows for a determination of L_{mnp} and Q_c. Not to belabor the point, Eq. (3) represents a local measure of the cavity's resonance, because the atoms in the cavity (frozen in place on the time scale of a Rabi period) sense the field strength in the particular region where the atomic-candle signal is generated and probed [22].[3]

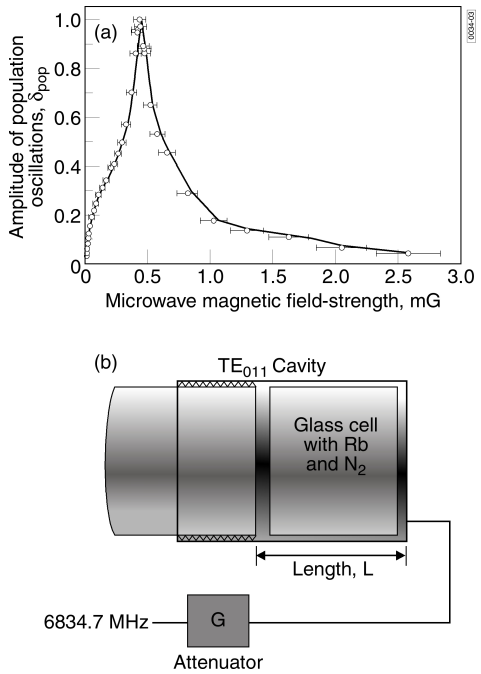

Figure 1: (a) Example of an atomic-cande-type Rabi-resonance lineshape as used in the present experiment. Note that when the atoms' experience a specific value of the microwave magnetic field strength, the amplitude of the modulation-induced atomic population oscillations increases dramatically. (b) Illustration of our use of the atomic-candle method to measure cavity resonance as discussed in the text.

2) Since cavity field strength varies linearly with the square root of the power fed, we calibrated our attenuator by taking advantage of the Rabi-resonance condition: G_{res} occurs when $B = B_{res} \equiv 2\hbar\omega_m/\mu_B$.

3) A number of years ago we developed an alternate method for measuring local field strengths in a cavity [22]. However, due to the resonant nature of the atomic-candle signal, the present method is likely more accurate

III. EXPERIMENTAL ARRANGEMENT

Figure 2 shows a block diagram of our experimental arrangement. Light from a diode laser was tuned to the Rb^{87} D_1 transition at 794.7 nm (i.e., $5^2S_{1/2}(F=2) - 5^2P_{1/2}(F'=1)$), attenuated by neutral density filters, and then expanded and apertured to a final diameter of 0.8 cm with I = 3.5 $\mu W/cm^2$. (Given the 520 MHz Doppler broadening of the optical transition, we were just able to resolve the 812 MHz splitting between the F'=1 and F'=2 hyperfine states). The laser beam passed into a resonance cell containing isotopically enriched Rb^{87} along with 10 torr N_2, which was housed in a cylindrical TE_{011} microwave cavity nearly resonant with the ground-state hyperfine transition at 6834.7 MHz. The copper microwave cavity was constructed in two pieces, so that a threaded end cap could be screwed in or out in order to change the cavity length.[4] Radially, the Corning 7070 resonance cell fit snugly into the cavity, and had a length of ~ 5.6 cm (i.e., L_o), a diameter, 2R, of 5.7 cm, and was heated with braided windings wrapped on the copper cavity body to about 35 ^oC corresponding to a Rb vapor density of ~ $6x10^{10}$ cm^{-3} [23]. The cavity and cell were centrally located in a set of three mutually perpendicular Helmholtz coils: two pairs zeroed out the Earth's residual magnetic field while the third provided a quantization axis for the atoms (i.e., z-axis) parallel to the laser propagation direction and cavity symmetry axis: $B_{z,DC}$ ~ 400 mG. Transmission of the light through the vapor was monitored with a Si photodiode.

In the absence of microwaves resonant with the (F=2, m_F=0) – (1,0) hyperfine transition (i.e., 0-0 transition), depopulation optical pumping reduced the density of atoms in the F=2 absorbing state [24], and consequently increased the amount of light transmitted through the vapor. However, when the resonant microwave signal was present atoms returned to the F=2 state, thereby reducing the amount of transmitted light. The transmitted laser intensity thus acted as a measure of atomic population in the F=2 level, so that any microwave induced oscillation of this population was observed as oscillations in the transmitted light and appeared as a "bright line" on the spectrum analyzer. Since our atomic-candle signal is associated with population oscillations occurring at $2\omega_m$ [13], we were able to measure δ_{pop} very easily by simply recording the amplitude of the bright line on the spectrum analyzer at $2\omega_m$. We note that Doppler broadening played no role in our experiments as a consequence of Dicke narrowing [25].

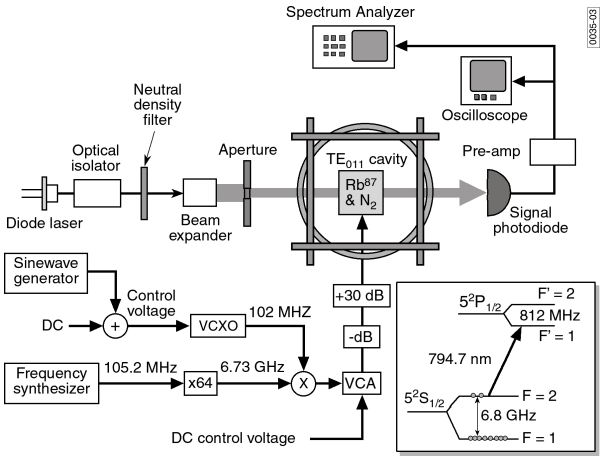

Figure 2: Experimental arrangement.

The microwaves were derived from a very low phase noise frequency synthesizer whose output at 105.2 MHz was multiplied up into the microwave regime and then mixed with the output of a voltage controlled crystal oscillator (VCXO) at ~ 102 MHz. The microwaves were attenuated by the combination of a voltage controlled attenuator (VCA) and a fixed attenuator (labeled as −dB in the figure) before being amplified by a +30 dB solid-state amplifier. A sinusoidal signal of frequency ω_m was added to a DC voltage in order to provide the VCXO's control voltage, V_c. The DC level of V_c tuned the average microwave frequency to the 0-0 hyperfine resonance, while the sine wave provided microwave frequency (i.e., phase, $\delta\theta$) modulation: $\delta\theta(t) = m\cos(\omega_m t)$. In these experiments, $\omega_m/2\pi$ = 328 Hz and the modulation index, m, was 0.74.

Prior to measuring the cavity resonance with the atomic-candle signal, we studied the cavity with a more traditional power-transmission technique. Basically, we used a directional coupler to measure the reflected microwave power from the cavity as a function of length, $P_r(L)$; then, defining P_o as the reflected power with the cavity off resonance, we approximated the transmitted power, $P_t(L)$, as the difference between P_o and $P_r(L)$. The solid line in Fig. 3 shows this transmitted power as a function of the cavity's detuning Δ_c from the 0-0 hyperfine resonant frequency. Basically, Δ_c is a parameter that re-expresses the cavity's length in terms of an appropriate cavity resonant frequency for that length:

4) We measured the change in cavity length per cylinder turn, and checked that this was consistent with the documented threading of the end cap.

$$\Delta_c \equiv \omega_{hfs} - c\sqrt{\left(\frac{x'_{mn}}{R}\right)^2 + \left(\frac{\pi p}{L}\right)^2} = \omega_{hfs} - \omega_c , \quad (4)$$

where L is the measured cavity length, and x'_{mn} is the n^{th} root of $J'_m(x) = 0$ with J'_m the derivative of an m^{th} order Bessel function [21]. For the TE_{011} mode, $x'_{mn} = 3.832$ and p = 1.

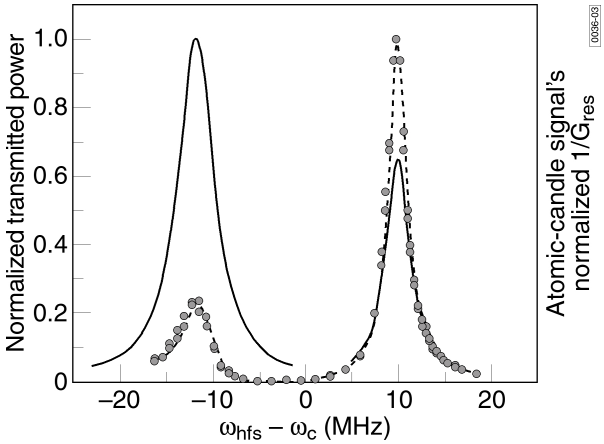

Figure 3: Cavity resonances. The solid line corresponds to the cavity resonance observed using the traditional power-transmission technique, while the circles correspond to the cavity resonance as observed using the atomic-candle method. As discussed in the text, the difference between these two curves is due to the local nature of the atomic-candle method as opposed to the global nature of the power-transmission method.

As the figure clearly shows, our cavity exhibits two resonances near 6.8 GHz separated by about 135 MHz.[5] The lower frequency resonance (i.e., $\Delta_c < 0$) has a Q_c of ~1500, while the higher frequency resonance has a Q_c of ~2200; moreover, the larger amplitude of the low frequency resonance implies that it is better able to couple microwave power into the cavity. In a separate set of experiments, where we examined the cavity without the resonance cell using the reflected power technique, we also observed these two resonances. For the empty cavity measurements we fixed the cavity length, scanned the input microwave frequency as we measured the reflected power, and thereby determined the resonant frequency for each of the modes at the specific cavity length. Repeating this procedure for a set of cavity lengths, we then fit the square of the resonant frequencies to $c^2\left[\left(\frac{x'_{mn}}{R}\right)^2 + \left(\frac{\pi p}{L}\right)^2\right]$, and obtained x'_{mn} and p values for each of the modes. We found that both cavity resonances were consistent with the TE_{011} parameters.[6] Based on computations of cavity field distributions, we believe that the 1.1 cm diameter holes in our cavity, which allow the laser light to enter and exit the cavity, cause the TE_{011} mode to split into a few "sub-modes." For future reference we will refer to the low frequency sub-mode as the TE^a_{011} mode and the higher frequency sub-mode as the TE^b_{011} mode.

Returning to the cavity experiments with the resonance cell, circles in Fig. 3 show our measurements of G_{res}^{-1} as a function of Δ_c using the atomic-candle method. Similar to the reflected power measurements, we see two sub-modes with the same widths and spacing.[7] The striking difference between these two measurement procedures is the asymmetry in the TE^a_{011} and TE^b_{011} modes' amplitudes. Specifically, for the atomic-candle method it appears that less gain is required by the TE^b_{011} mode in order to produce a given value of cavity field strength, implying that this mode is better able to couple microwaves into the cavity. This observation would seem to be at odds with the results from the power-transmission method. To resolve this discrepancy, we note that the laser only probes atoms very near the cavity axis (i.e., R = 2.9 cm, r_{laser} = 0.4 cm), and that the atomic-candle method provides a local determination of the cavity's modal features. Consequently, though the TE^a_{011} mode is *globally* more efficient at coupling power into the cavity, the TE^b_{011} mode appears more efficient at *localizing* the axial component of the microwave magnetic field in the central regions of the cavity where the atoms are probed. Here, then, we have a rather serendipitous and dramatic demonstration of the atomic-candle method's utility for cavity resonance measurements. Specifically, when coupled with a more traditional method, the local nature of the atomic-candle method can "tease out" information on a cavity mode's spatial profile.

5) For illustrative purposes, we have chosen the zero of Δ_c so that the two cavity resonances appear nearly symmetrical about $\Delta_c = 0$.

6) For the lower frequency resonance we found $x'_{mn} = 3.77 \pm 0.02$ and $p = 1.04 \pm 0.02$, while for the higher frequency resonance we found $x'_{mn} = 3.895 \pm 0.002$ and $p = 0.981 \pm 0.003$.

7) Using the atomic-candle method, $Q_c \sim 1700$ for the TE^a_{011} mode, while $Q_c \sim 2700$ for the TE^b_{011}.

IV. CAVITY TEMPORAL VARIATIONS

As suggested in the Introduction, our primary motivation for initiating these studies was to investigate temporal changes in the resonant frequency and quality factor of a gas-cell atomic clock's microwave cavity. We hypothesized that due to a slow redistribution of alkali metal within the resonance cell over long periods of time, Q_c and/or ω_c might "age." To test this hypothesis, we removed our glass resonance cell from the cavity, and "drove down" the rubidium condensed phase to one end of the cell.[8] Briefly, we wrapped heating wire around the sides and top of the cell and heated this to about 60 °C. Additionally, we placed heat sink putty on the cell's "pull-off" tip (i.e., the small cylindrical protrusion from the body of the cell where the cell had been attached to a glass vacuum system during its fabrication.), and connected this to a metal table separated from the rest of the cell by a piece of foam. We cooled the table down by placing dry ice on it, and were thereby able to obtain a temperature gradient across the cell of something close to 140 °C, which we maintained for ~ 12 hours. After the dry ice evaporated, the temperature gradient across the cell was roughly 40 °C. (The drive-down procedure took place over the weekend, when the laboratory was unoccupied.) Though we could not observe a liquid phase of the alkali in our cell (there was too little isotopically enriched rubidium in the relatively large cell for easy visualization) we knew that a condensed phase must exist, because the Rb vapor density in our cell depended on temperature as expected for a liquid/vapor equilibrium [26]. Since the condensed phase must move to the cell's cold point for a vapor in equilibrium with the condensed phase, we assumed that after 60 hours nearly all of the Rb had collected in our cell's tip.

Following the drive down procedure, we placed the resonance cell in the cavity; heated the cell up to 35 °C, and began a series of measurements on the TE^b_{011} mode's resonant frequency and Q. These are shown in Fig. 4 by the open triangles and circles, respectively. While we saw no change in the mode's resonant frequency, there was a very noticeable change in the cavity mode's Q. The solid line is a least squares fit of the data to an exponential form:

$$Q_c(t) = Q_o + \delta Q e^{-t/\tau}, \qquad (5)$$

and we find $Q_o = 1495$, $\delta Q = 1255$ and $\tau = 67$ days. At day 52, we halted the experiment, removed the resonance cell from the cavity, and repeated the exact same drive-down procedure. We then placed the resonance cell back in the cavity at 35 °C and continued our measurements of the TE^b_{011} mode's resonant frequency and quality factor; these are shown as filled triangles and circles, respectively, in Fig. 4. As the data clearly show, though the resonant frequency was unaffected by the second drive down, the cavity Q recovered to its initial value.

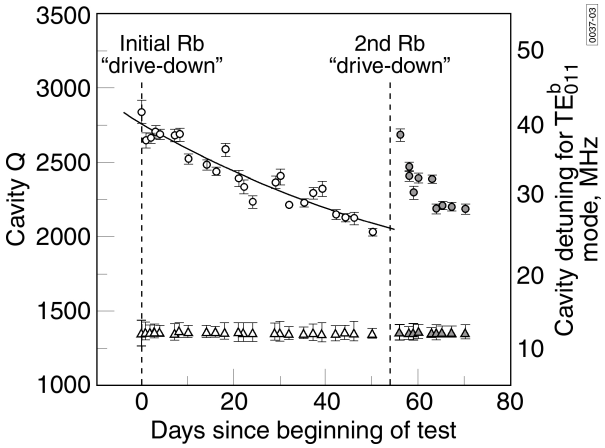

Figure 4: Cavity-Q and resonant-frequency aging in our microwave cavity: open symbols correspond to data following the first drive down, while filled symbols correspond to data following the second drive down; circles correspond to cavity Q, while triangles correspond to the cavity's resonant frequency.

We hypothesize that the cavity-Q's decay is due to a redistribution of condensed phase Rb within the resonance cell, perhaps in the form of a film coating the inside glass surface. Several lines of argument lead us to this conclusion. First, whatever the mechanism responsible for the cavity-Q's decay, it cannot be associated with a change in the electrical dimensions of the cavity/resonance-cell, otherwise the cavity detuning corresponding to the TE^b_{011} mode would have changed during the course of the experiment. Further, since we had observed that the cavity Q depended on the placement of the resonance cell within the cavity, at one point we were tempted to explain the decay as arising from resonance-cell "creep" within the cavity (i.e., over a period of days, the resonance cell might undergo a mechanical relaxation of its position within the cavity). However, for each data point shown in Fig. 4, we obtained the TE^b_{011} mode lineshape by increasing the cavity length from "zero," which corresponded to the cavity ends just touching the glass resonance cell. This had the effect of repositioning the resonance cell in the cavity for each of the data points,

8) Prior to this drive-down procedure, the cavity and resonance cell had been maintained at 62 °C for nearly a week.

thereby eliminating any effect of creep over the long-term test. In fact, we believe that some of the variability among the data points shown in Fig. 4 may be due to this repositioning. Finally, the cavity-Q's recovery to its initial value following the second drive down argues forcefully for an alkali redistribution effect. Even the relatively fast (i.e., $\tau \sim 10$ days) cavity-Q decay after the second drive down is consistent with the evolution of an alkali film. Since surface diffusion coefficients can change by orders of magnitude depending on the relative surface coverage [27], it is not difficult to imagine that there were differences in the initial surface coverage following the first and second drive-down procedures given the differences in the resonance-cell's history in the two cases. We also note that the anticipated time scale for cavity-Q degradation due to film evolution is consistent with our findings: given that surface diffusion coefficients can be on the order of 10^{-5} cm^2/s [28], our resonance cell surface area of 10^2 cm^2 would imply a multi-month time constant for complete coverage.

V. Consequences for Clock Frequency Aging

As already mentioned, changes in the cavity Q of a gas-cell clock will affect the clock's frequency as a result of the position-shift and/or cavity-pulling effects. In this Section, we want to estimate the magnitude of these effects for a clock based on the present experiment's TE^b_{011} mode. Though we recognize that our cavity Q is roughly a factor of 5 to 10 times larger than that of typical clocks, the present exercise nonetheless has merit since it places an upper bound on the frequency variations that might occur in these devices. As shown below, this upper bound is actually quite large, and suggests that cavity-Q variations may play a role in the long-term stability of Rb atomic clocks.

According to Sarosy et al. [29], the position-shift effect's dependence on microwave power in commercial Rb frequency standards can be as large as $3\text{x}10^{-11}$/dB. However, physical considerations lead us to expect the position-shift to depend not so much on the input power, P, but on the energy density, E, within the cavity. We therefore expand the atomic clock's frequency, ω_{clk}, in a Taylor series about the nominal cavity energy density, E_o, to obtain $\delta\omega_{clk} = \left.\frac{\partial\omega_{clk}}{\partial E}\right|_{E=E_o} \delta E$. Since the energy density scales like Q_cP, $\delta E \sim Q_c\delta P + P\delta Q_c$, and so the fractional change in the position-shift due to a microwave power or cavity-Q variation, $\delta[\Delta y_{position}]$, may be written as

$$\delta\left[\Delta y_{position}\right] = \frac{E_o}{\omega_{clk}} \left.\frac{\partial\omega_{clk}}{\partial E}\right|_{E=E_o} \left(\frac{\delta P}{P_c} + \frac{\delta Q}{Q_c}\right). \quad (6)$$

Based on the results of Sarosy et al. [29], a 0.23 relative change in microwave power can give rise to a $3\text{x}10^{-11}$ fractional frequency change, implying that

$$\frac{E_o}{\omega_{clk}} \left.\frac{\partial\omega_{clk}}{\partial E}\right|_{E=E_o} = 1.3\text{x}10^{-10}. \quad (7)$$

Thus, we expect $\delta[\Delta y_{position}] \sim 10^{-10}(\delta Q/Q_c)$.

The fractional frequency shift due to cavity pulling can be written as

$$\Delta y_{pull} = \frac{\alpha Q_c\left(\omega_c - \omega_{hfs}\right)}{\omega_{hfs} Q_a \left(1+S\right)}, \quad (8)$$

where α is a parameter representing the degree of coupling between the atoms and the cavity; S is a saturation parameter, and Q_a is the atoms' quality factor [3,6]. In gas cell clocks, $\alpha \sim 10^{-2}$, S ~ 2, and $Q_a \sim 10^7$; thus, for a relative cavity detuning on the order of Q_c^{-1}, $\delta[\Delta y_{pull}] \sim 3\text{x}10^{-10}(\delta Q/Q_c)$. Thus, the position-shift and cavity-pulling effects can be of the same order of magnitude, and we therefore express the upper bound on frequency aging due to cavity-Q variations as

$$\frac{\delta\omega_{clk}(t)}{\omega_{clk}} \sim 4\text{x}10^{-10} \frac{\delta Q(t)}{Q_c}. \quad (7)$$

Substituting from Eq. (5), we get a cavity-Q induced frequency-aging rate of roughly $3\text{x}10^{-12}$/day at short times t, just after a clock's turn-on. This is of the same order of magnitude as a recent measurement of initial frequency aging in a high-quality Rb clock onboard a geostationary satellite, and more than an order-of-magnitude larger than the clock's eventual quiescent frequency aging rate [30].

VI. Summary

We have employed an atomic-candle signal to investigate the long-term aging of a gas-cell clock's microwave cavity, and for the first time have obtained evidence pointing to a role for alkali redistribution (within the resonance cell) in the gas-cell clock's frequency stability. Additional work in this area is certainly warranted. In particular, there is a lack of knowledge regarding alkali surface diffusion on various types of glass, and given the present findings this could be a very fruitful area of investigation. Moreover, we have found that when our atomic-candle

method is combined with more traditional methods, the combination has the potential to yield information on spatial mode profiles within the cavity. Consequently, while we have employed the atomic-candle method to investigate cavity resonances in the specific case of the rubidium atomic clock, we believe that the method will have much wider applicability.

ACKNOWLEDGMENTS

The author would like to thank J. Coffer, B. Sickmiller and A. Presser for assistance in performing the experiments, and S. Moss for stimulating discussions regarding surface diffusion. This work was supported by U.S. Air Force Space and Missile Systems Center under Contract No. F040701-00-C-0009.

APPENDIX

Regarding the position-shift effect, the atoms giving rise to the clock's signal are enclosed within a glass resonance cell that is contained inside a resonant microwave cavity, which in turn is situated inside a (dc) magnetic-field producing solenoid. Due to the presence of a buffer gas at tens of torr pressure (e.g., N_2), the vapor-phase alkali atoms are effectively frozen in place on the time scale of a Rabi period, so that the atoms primarily responsible for the clock's signal are confined to a relatively small region of space. The location of this region is determined by a complicated interplay between the microwave field's and the optical-pumping light's spatial distributions, as well as the resonance cell geometry [31]. As a consequence of this confinement, the clock's output frequency is strongly influenced by local perturbations acting on the atoms; in particular, localized values of the quadratic Zeeman shift [32] and ac-Stark shift [33,34]. When the microwave field strength within the clock's cavity varies, as a result of changes in the cavity's electrical characteristics or changes in the microwave power, the primary signal-producing region will move to a new location with different local perturbations, giving rise to a shift in the clock's output frequency that can be fairly large.

Concerning the cavity-pulling effect, in the case of a mistuned cavity the microwave field strength will be greater on one side of resonance than on the other. As a result, the atoms' peak response to the microwaves will occur when the microwave field is slightly detuned from the Rb^{87} atom's ground-state hyperfine resonant frequency.

REFERENCES

1. A. Risley and G. Busca, "Effect of line inhomogeneity on the frequency of passive Rb^{87} frequency standards," in Proc. 32nd Annual Sym. Freq. Control (Electronic Industries Assoc., Atlantic City NJ, 1978) pp. 506-513.
2. A. Risley, S. Jarvis, and J. Vanier, "The dependence of frequency upon microwave power of wall-coated and buffer-gas-filled gas cell Rb^{87} frequency standards," *J. Appl. Phys*, vol. 51, pp. 4571-4576, 1980.
3. J. Vanier and C. Audoin, The Quantum Physics of Atomic Frequency Standards: Vol.2 (Adam Hilger, Bristol, 1989) pp. 1205-1211.
4. J. C. Camparo, "A partial analysis of drift in the rubidium gas cell atomic clock," in Proc. 18th Annual Precise Time and Time Interval (PTTI) Applications and Planning Meeting (Naval Observatory, Washington DC, 1986) pp. 565-588.
5. W. J. Riley, "The physics of the environmental sensitivity of rubidium gas cell atomic frequency standards," in Proc. 22nd Annual Precise Time and Time Interval (PTTI) Applications and Planning Meeting (Naval Observatory, Washington DC, 1990) pp. 441-452.
6. J. Viennet, C. Audoin, and M. Desaintfuscien, "Cavity pulling in passive frequency standards," *IEEE Trans. Instrum. Meas.*, vol. 21, pp. 204-209, 1972.
7. X. Huang, B. Xia, D. Zhong, S. An, X. Zhu, and G. Mei, "A microwave cavity with low temperature coefficient for passive rubidium frequency standards," in Proc. 2001 IEEE Internat. Freq. Control Symp. & PDA Exhibition (IEEE Press, Piscataway NJ, 2001) pp. 105-107.
8. H. E. Williams, T. M. Kwon, and T. McClelland, "Compact rectangular cavity for rubidium vapor cell frequency standards," in Proc. 37th Annual Symp. Freq. Control (IEEE Press, Piscataway NJ, 1983) pp. 12-17.
9. E. Eltsufin, A. Stern, and S. Fel, "Compact rectangular-cylindrical cavity for rubidium frequency standard," in Proc. 45th Annual Symp. Freq. Control (IEEE Press, Piscataway NJ, 1991) pp. 567-571.
10. J. Deng, "Subminiature microwave cavity for atomic frequency standards," in Proc. 2001 IEEE Internat. Freq. Control Symp. & PDA Exhibition (IEEE Press, Piscataway NJ, 2001) pp. 85-88.
11. L. B. Young, "Frequency measurements," in Technique of Microwave Measurements, ed. C. G. Montgomery (McGraw-Hill, New York, 1947), Ch. 6.
12. J. C. Camparo, "Magnetic resonance in cesium vapor: Detection of photoinduced paramagnetic species and spin exchange amplification of rf broadening," Ph.D. thesis, Columbia University, 1981.
13. J. G. Coffer, B. Sickmiller, A. Presser, and J. C. Camparo, "Line shapes of atomic-candle-type

Rabi resonances," *Phys. Rev. A*, vol. 66, 023806, 2002.
14. T. Swan-Wood, J. G. Coffer and J. C. Camparo, "Precision measurements of absorption and refractive-index using an atomic candle," *IEEE Trans. Instrum. Meas.*, vol. 50, pp. 1229-1233, 2001.
15. E. L. Ginzton, Microwave Measurements (McGraw-Hill, New York, 1957) Ch. 9.
16. U. Cappeller and H. Mueller, "Phase modulated excitation on optically pumped spin system," *Ann. der Phys. (Leipzig)*, vol. 42, pp. 250-264, 1985.
17. R. P. Frueholz and J. C. Camparo, "Entropy and attractor dimension as measures of the field-atom interaction," *Phys. Rev. A*, vol. 47, pp. 4404-4411, 1993.
18. J. C. Camparo and J. G. Coffer, "Accessing photon number via an atomic time interval," *Phys. Rev. A*, vol. 66, 043416, 2002.
19. J. C. Camparo, "Atomic stabilization of electromagnetic field strength using Rabi resonances," *Phys. Rev. Lett.*, vol. 80, pp. 222-225, 1998.
20. J. G. Coffer and J. C. Camparo, "Atomic stabilization of field intensity using Rabi resonances," *Phys. Rev. A*, vol. 62, 013812, 2000.
21. J. D. Jackson, Classical Electrodynamics (John Wiley, New York, 1975) Ch. 8.
22. R. P. Frueholz and J. C. Camparo, "Microwave field strength measurement in a rubidium clock cavity via adiabatic rapid passage," *J. Appl. Phys.*, vol. 57, pp. 704-708, 1985.
23. T. J. Killian, "Thermionic phenomena caused by vapors of rubidium and potassium," *Phys. Rev.*, vol. 27, pp. 578-587, 1926.
24. W. Happer, "Optical pumping," *Rev. Mod. Phys.*, vol. 44, 169-249, 1972.
25. R. H. Dicke, "The effect of collisions upon the Doppler width of spectral lines," *Phys. Rev.*, vol. 89, pp. 472-473, 1953; R. P. Frueholz and C. H. Volk, "Analysis of Dicke narrowing in wall-coated and buffer-gas-filled atomic storage cells," *J. Phys. B: At. Mol. Phys.*, vol. 18, pp. 4055-4067, 1985.
26. G. W. Castellan, Physical Chemistry (Addison-Wesley, Reading, MA, 1971) Ch. 11.
27. A. G. Naumovets and Z. Zhang, "Fidgety particles on surfaces: How do they jump, walk, group, and settle in virgin areas," *Surf. Sci.*, 500, pp. 414-436, 2002.
28. See for example: S. Garofalini, "Potassium diffusion at the surface of a $K_2O{\cdot}3SiO_2$ glass," *J. Vac. Sci. Technol. A*, vol. 2, pp. 79-81, 1984; A. P. Graham and J. P. Toennies, "Macroscopic diffusion and low-frequency vibrations of sodium on Pt(111) investigated with helium atom scattering," *J. Phys. Chem. B*, vol. 105, pp. 4003-4009, 2001; P. S. Maiya and J. M. Blakely, "Surface self-diffusion and surface energy of nickel," *J. Appl. Phys.*, vol. 38, pp. 698-704, 1967.
29. 1. E. B. Sarosy, W. A. Johnson, S. K. Karuza, and F. Voit, "Measuring frequency changes due to microwave power variations as a function of C-field setting in a rubidium frequency standard," in Proc. 23rd Annual Precise Time and Time Interval (PTTI) Applications and Planning Meeting (U.S. Naval Observatory, Washington, D.C., 1991) pp. 229-235.
30. J. G. Coffer and J. C. Camparo, "Long-term stability of a rubidium atomic clock in geosynchronous orbit," in Proc. 31st Annual Precise Time and Time Interval (PTTI) Systems and Applications Meeting (US Naval Observatory, Washington DC, 2000) pp. 65-74.
31. J. C. Camparo and R. P. Frueholz, "A three-dimensional model of the gas cell atomic frequency standard," *IEEE Trans. Ultrason. Ferroelec. Freq. Control*, vol. 36, pp. 185-190, 1989.
32. J. Vanier and C. Audoin, The Quantum Physics of Atomic Frequency Standards: Volume 1 (Adam Hilger, Bristol, England, 1989) Ch.1.
33. B. S. Mathur, H. Tang, and W. Happer, "Light shifts in the alkali atoms," *Phys. Rev.*, vol. 171, pp. 11-19, 1968.
34. J. C. Camparo, R. P. Frueholz, and C. H. Volk, "Inhomogeneous light shift in alkali-metal atoms," *Phys. Rev. A*, vol. 27, pp. 1914-1924, 1983.